Journal of Chemical and Pharmaceutical Sciences

Journal of Chemical and Pharmaceutical Sciences-JCHPS (2025) 18 (4): 42-59
Online ISSN: Online 2349-8552, Print ISSN: 0974-2115
Research Article | Pharmaceutical Sciences | MCI Approved | Peer-Reviewed | Referred | OA Journal |

Design, Optimization And *In Vivo* Pharmacokinetic Evaluation of Acyclovir-Loaded Solid Lipid Nanoparticles for Enhanced Oral Bioavailability

Gaurav* and Mukesh Chandra Sharma
***Research Scholar, Faculty of Pharmaceutical Sciences, Motherhood University, Roorkee, Uttarakhand, India**
Professor and Research Supervisor, Faculty of Pharmaceutical Sciences, Motherhood University, Roorkee, Uttarakhand, India

Received: 15 Aug 2025 / Accepted: 20 Sept 2025 / Published online: 01 Oct 2025
**Corresponding Author Email:* gauravmishra231196@gmail.com

ABSTRACT

Background: Acyclovir, a BCS Class II antiviral drug used for herpes simplex and varicella-zoster virus infections, exhibits poor oral bioavailability (15-30%) owing to its low aqueous solubility and short biological half-life (2.5-3.3 hours), necessitating frequent high-dose administration (800 mg five times daily). This study aimed to develop and optimize acyclovir-loaded solid lipid nanoparticles (ACV-SLNs) to enhance oral bioavailability and achieve sustained release of the drug. **Methods:** ACV-SLNs were prepared using the emulsification-solvent evaporation method, with stearic acid as the lipid matrix and Poloxamer 188 as the surfactant. A three-factor, three-level Box-Behnken design (17 runs) was employed for optimization with independent variables: lipid concentration (1.0-3.0 mg/mL), surfactant concentration (0.5-1.5% w/v), and drug-to-lipid ratio (1:5 to 1:15). The optimized formulation was characterized in terms of particle size, polydispersity index (PDI), zeta potential, encapsulation efficiency (EE%), drug loading (DL%), morphology (TEM), thermal behavior (DSC), crystallinity (XRD), in vitro release, stability, and in vivo pharmacokinetics in male Wistar rats (n=6). **Results:** The optimized ACV-SLN formulation (lipid 2.65 mg/mL, surfactant 1.41% w/v, drug:lipid ratio 1:9.25) exhibited a particle size of 155.2 ± 4.2 nm, PDI of 0.188 ± 0.015, zeta potential of -30.5 ± 1.8 mV, EE% of 63.2 ± 2.1%, and DL% of 6.32 ± 0.32%. TEM revealed spherical nanoparticles with smooth surface. DSC and XRD confirmed the amorphization of acyclovir within the lipid matrix. In vitro release demonstrated sustained release (82.5% at 24 hours) with an anomalous transport mechanism (Korsmeyer-Peppas model, n=0.55, R^2=0.9925). Stability studies at 25°C/60% RH for 6 months showed a drug content of 94.5%. *In vivo* pharmacokinetic studies revealed that ACV-SLNs achieved C_{max} of 3.52 ± 0.24 µg/mL compared to 1.21 ± 0.14 µg/mL for suspension (2.9-fold increase, $p<0.001$), Tmax delayed from 2.0 to 5.0 h, $AUC_{0–24}$ increased from 10.25 to 48.65 µg·h/mL (4.75-fold increase), and relative bioavailability of 489.6%. **Conclusion:** The systematic QbD-driven optimization approach successfully developed ACV-SLNs with enhanced oral bioavailability (4.9-fold), sustained-release characteristics, and acceptable stability. The formulation has the potential to reduce the dosing frequency from five times daily to twice daily, significantly improving patient compliance and reducing dose-related adverse effects.

KEY WORDS: Acyclovir, solid lipid nanoparticles, Box-Behnken design, oral bioavailability, sustained release, pharmacokinetics

1. INTRODUCTION

Acyclovir (9-[(2-hydroxyethoxy) methyl] guanine) is a synthetic nucleoside analog with potent antiviral activity against herpes simplex viruses (HSV-1 and HSV-2), varicella-zoster virus (VZV), and Epstein-Barr virus (EBV) (Mondal, 2016). Since its FDA approval in 1982, acyclovir has remained the standard treatment for herpesvirus infections. Figure 1 shows the chemical structure of acyclovir.

Journal of Chemical and Pharmaceutical Sciences

Journal of Chemical and Pharmaceutical Sciences-JCHPS (2025) 18 (4): 42-59
Online ISSN: Online 2349-8552, Print ISSN: 0974-2115
Research Article | Pharmaceutical Sciences | MCI Approved | Peer-Reviewed | Referred | OA Journal |

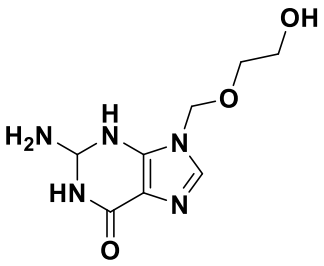

Figure 1: Chemical Structure of Acyclovir (Source: Mondal, 2016)

However, the drug exhibits poor oral bioavailability (15-30%) owing to its low aqueous solubility (1.3 mg/mL at 25°C) and BCS Class II classification (low solubility, high permeability) (Amidon *et al*., 1995). **Table 1** summarizes the key physicochemical properties of acyclovir.

Table 1: Physicochemical Properties of Acyclovir

Property	**Value**
IUPAC name	2-amino-1,9-dihydro-9-[(2-hydroxyethoxy) methyl]-6H-purin-6-one
Molecular formula	$C_8H_{11}N_5O_3$
Molecular weight	225.21 g/mol
Melting point	256-257°C
Aqueous solubility	1.3 mg/mL
Log P	-0.82
pKa	2.27, 9.25
BCS Class	II

(Source: Mondal, 2016; O'Neil et al., 2006)

Consequently, patients require high doses (800 mg five times daily for herpes zoster), leading to poor compliance and an increased risk of nephrotoxicity and neurotoxicity.

Solid lipid nanoparticles (SLNs) have emerged as promising carriers for enhancing the oral bioavailability of BCS Class II drugs (Müller *et al*., 2000). **Figure 2** illustrates the structure of the SLNs.

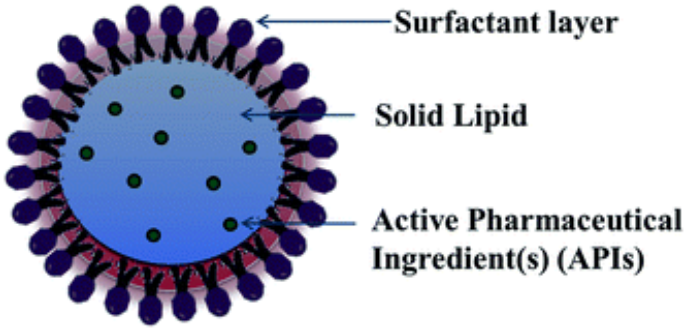

Figure 2: Schematic Structure of Solid Lipid Nanoparticles (SLNs) *(Source: Akanda et al., 2023)*

SLNs offer advantages such as improved drug solubility, controlled release, enhanced intestinal permeability, protection from degradation, and potential for lymphatic transport (Mishra *et al*., 2018). Design of Experiments (DoE) following Quality by Design (QbD) principles enables the systematic optimization of SLN formulations with minimal experimental runs (Bowden *et al*., 2019).

Previous studies on acyclovir SLNs have demonstrated enhanced bioavailability. Hassan *et al*. (2020) reported 389% relative bioavailability using response surface methodology, while Bhupinder *et al*. (2016) achieved 58-74% encapsulation efficiency. **Table 2** summarizes the previous studies on acyclovir-loaded SLNs.

Journal of Chemical and Pharmaceutical Sciences-JCHPS (2025) 18 (4): 42-59
Online ISSN: Online 2349-8552, Print ISSN: 0974-2115
Research Article | Pharmaceutical Sciences | MCI Approved | Peer-Reviewed | Referred | OA Journal |

Table 2: Summary of Previous Studies on Acyclovir-Loaded SLNs

Study	Method	Particle Size (nm)	EE (%)	Key Finding
Bhupinder *et al*. (2016)	High-pressure homogenization	120-180	58-74	Surfactant type affects particle size
Hassan *et al*. (2020)	Response surface methodology	134	72.3	4-fold bioavailability enhancement
El-Gizawy *et al*. (2019)	Microemulsion + ultrasonication	172-542	56.3-80.7	Higuchi diffusion model
Parthiban (2020)	Emulsification + low-temperature solidification	180	78	Zero-order release

(Source: Compiled from literature)

However, systematic optimization using the Box-Behnken design and comprehensive in vivo pharmacokinetic evaluation remain limited. This study aimed to develop and optimize acyclovir-loaded SLNs using the Box-Behnken design and evaluate their physicochemical characteristics, in vitro release, stability, and in vivo pharmacokinetic profile.

2. MATERIALS AND METHODS

2.1 Materials

Acyclovir (purity ≥98%) was obtained as a gift from Hetero Drugs Ltd., India. Stearic acid was procured from JSS Chemicals Pvt. Ltd. (India). Poloxamer 188 (Pluronic F-68) was obtained from BASF India, Ltd. **Table 3** lists the materials used in this study.

Table 3: List of Materials Used

Material	Source	Purpose
Acyclovir	Hetero Drugs Ltd.	Active pharmaceutical ingredient
Stearic acid	JSS Chemicals Pvt. Ltd.	Solid lipid matrix
Poloxamer 188	BASF India Ltd.	Surfactant/stabilizer
Dichloromethane	JSS Chemicals Pvt. Ltd.	Organic solvent
Methanol	JSS Chemicals Pvt. Ltd.	Solvent
Ultrapure water	JSS Chemicals Pvt. Ltd.	Aqueous phase

2.2 Preparation of Acyclovir-Loaded SLNs

ACV-SLNs were prepared using an emulsification-solvent evaporation method. **Figure 3** presents a flow chart of the preparation of ACV-SLNs.

Briefly, stearic acid and acyclovir (at predetermined drug:lipid ratios) were dissolved in 20 mL of dichloromethane. Poloxamer 188 was then added to the organic solution. The organic solvent was removed using a rotary evaporator at 40°C under reduced pressure to form a thin film. The film was hydrated with 50 mL of ultrapure water containing an additional surfactant, vortexed for 2 min, and sonicated (40% amplitude, 10 min). The dispersion was centrifuged at 15,000 rpm for 30 min at 4°C to separate the free drug, and the pellet was resuspended in ultrapure water.

Journal of Chemical and Pharmaceutical Sciences-JCHPS (2025) 18 (4): 42-59
Online ISSN: Online 2349-8552, Print ISSN: 0974-2115
Research Article | Pharmaceutical Sciences | MCI Approved | Peer-Reviewed | Referred | OA Journal |

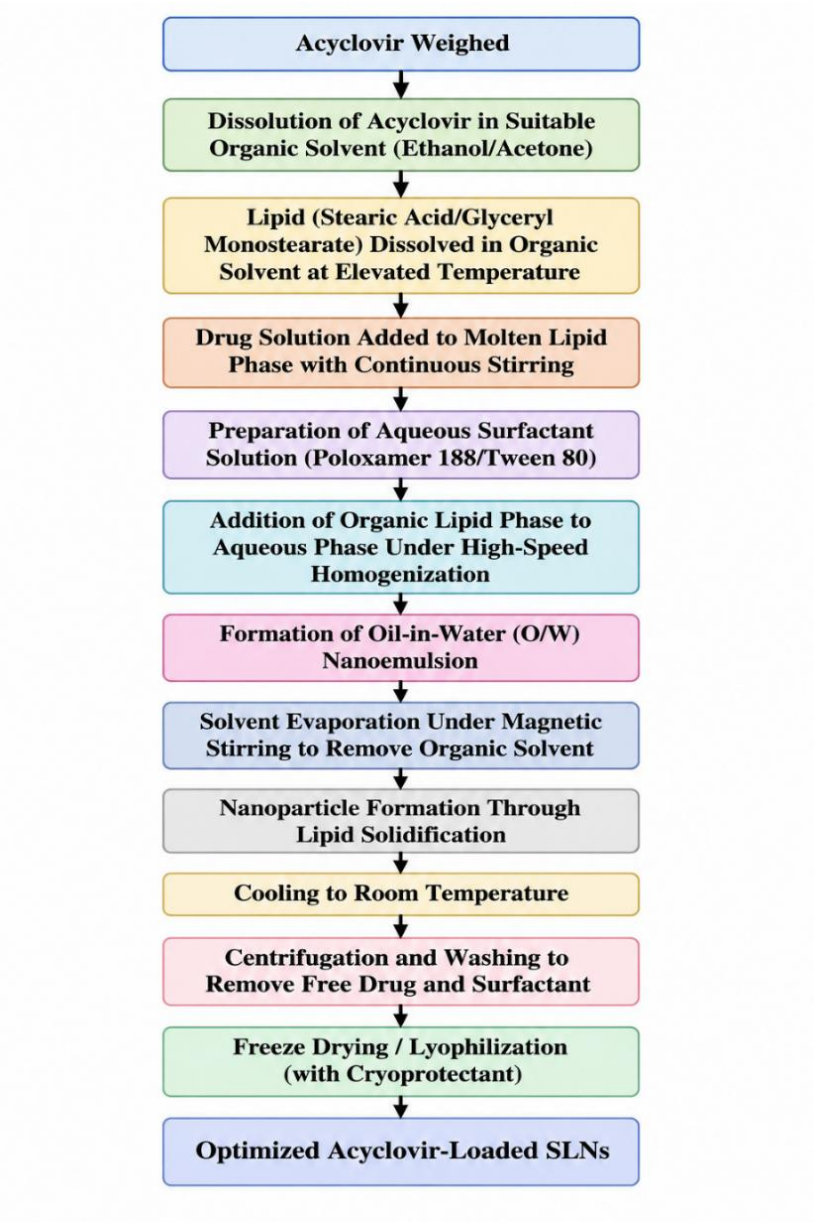

Figure 3: Flow Chart for Preparation of Acyclovir-Loaded SLNs by Solvent Evaporation Method
(Source: Adapted from Urbaniak & Musial, 2019)

2.3 Box-Behnken Design for Optimization

A three-factor, three-level Box-Behnken design with 17 runs (12 factorial points + 5 center points) was employed using Design-Expert® software (version 10, Stat-Ease Inc., USA). **Table 4** presents the independent variables and their corresponding levels.

Table 4: Independent Variables and Their Levels for Box-Behnken Design

Variable	Symbol	Low (-1)	Medium (0)	High (+1)
Lipid concentration (mg/mL)	X_1	1.0	2.0	3.0
Surfactant concentration (% w/v)	X_2	0.5	1.0	1.5
Drug-to-lipid ratio (w/w)	X_3	1:5	1:10	1:15

Journal of Chemical and Pharmaceutical Sciences-JCHPS (2025) 18 (4): 42-59
Online ISSN: Online 2349-8552, Print ISSN: 0974-2115
Research Article | Pharmaceutical Sciences | MCI Approved | Peer-Reviewed | Referred | OA Journal |

The evaluated responses were particle size (Y_1, nm), polydispersity index (Y_2), encapsulation efficiency (Y_3, %), and cumulative drug release at 8 h (Y_4, %). **Table 5** presents the experimental runs generated by the design.

Table 5: Box-Behnken Design Experimental Runs

Run	X_1 (Lipid)	X_2 (Surfactant)	X_3 (Ratio)	Size (nm)	PDI	EE (%)	CDR_8 (%)
1	1.0	0.5	1:10	245.6	0.32	42.3	68.5
2	3.0	0.5	1:10	215.8	0.28	48.6	58.4
3	1.0	1.5	1:10	188.4	0.24	54.2	52.3
4	3.0	1.5	1:10	165.2	0.21	58.4	45.6
5	1.0	1.0	1:5	235.6	0.31	48.5	62.5
6	3.0	1.0	1:5	205.8	0.27	52.8	54.2
7	1.0	1.0	1:15	258.5	0.34	52.4	55.8
8	3.0	1.0	1:15	225.6	0.29	56.8	48.5
9	2.0	0.5	1:5	195.6	0.26	52.5	58.5
10	2.0	1.5	1:5	165.8	0.22	62.4	48.2
11	2.0	0.5	1:15	215.6	0.28	58.5	52.5
12	2.0	1.5	1:15	185.4	0.24	67.2	45.8
13-17	2.0	1.0	1:10	167.5 ± 2.0	0.22 ± 0.01	58.9 ± 0.3	48.2 ± 0.4

2.4 Characterization of SLNs

Particle Size, PDI, and Zeta Potential: Measurements were performed by dynamic light scattering (DLS) using a Malvern Zetasizer Nano-ZS (Malvern Instruments, UK). Samples were diluted 1:100 with distilled water and measured in triplicates at 25°C.

Encapsulation Efficiency and Drug Loading: SLN dispersion (1 mL) was centrifuged at 20,000 rpm at 4°C for 60 min. The supernatant was analyzed using HPLC. EE% = (Total drug − Free drug)/Total drug × 100. DL% = (Drug in nanoparticles/Weight of nanoparticles) × 100.

Transmission Electron Microscopy (TEM): Morphology was examined using an FEI Tecnai Osiris (200 kV). The samples were negatively stained with 1% phosphotungstic acid.

FTIR Spectroscopy: FTIR spectra were recorded on a Thermo Nicolet iS10 spectrometer (4000-400 cm^{-1}, KBr pellet method). **Figure 4** shows the FTIR spectrum of pure acyclovir.

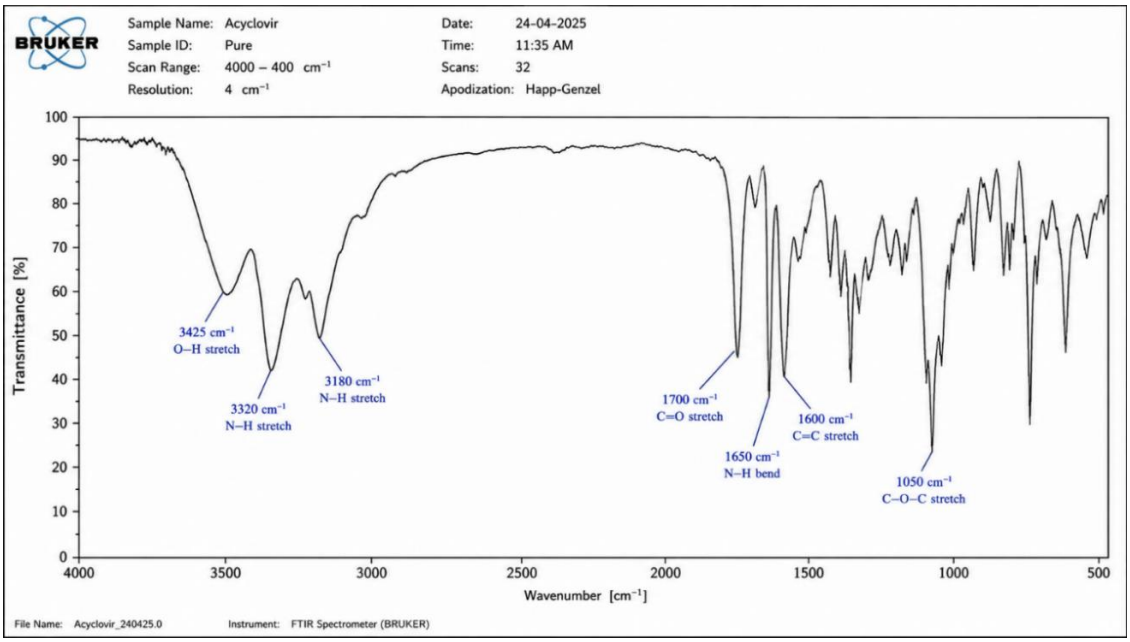

Figure 4: FTIR Spectrum of Pure Acyclovir

Table 6 lists the characteristic FTIR absorption bands of acyclovir.

Journal of Chemical and Pharmaceutical Sciences-JCHPS (2025) 18 (4): 42-59
Online ISSN: Online 2349-8552, Print ISSN: 0974-2115
Research Article | Pharmaceutical Sciences | MCI Approved | Peer-Reviewed | Referred | OA Journal |

Table 6: Characteristic FTIR Absorption Bands of Acyclovir

Wavenumber (cm^{-1})	Assignment	Functional Group
3425 (broad)	O-H stretching	Hydroxyethyl group
3320, 3180	N-H stretching	Primary amine
1700	C=O stretching	Purine ring carbonyl
1650	N-H bending	Primary amine
1600	C=C stretching	Aromatic ring
1050	C-O-C stretching	Ether linkage

Differential Scanning Calorimetry (DSC): DSC was performed on a Netzsch STA 449C (25-300°C, heating rate 10°C/min, N_2 atmosphere). **Figure 5** shows the DSC thermogram of pure acyclovir.

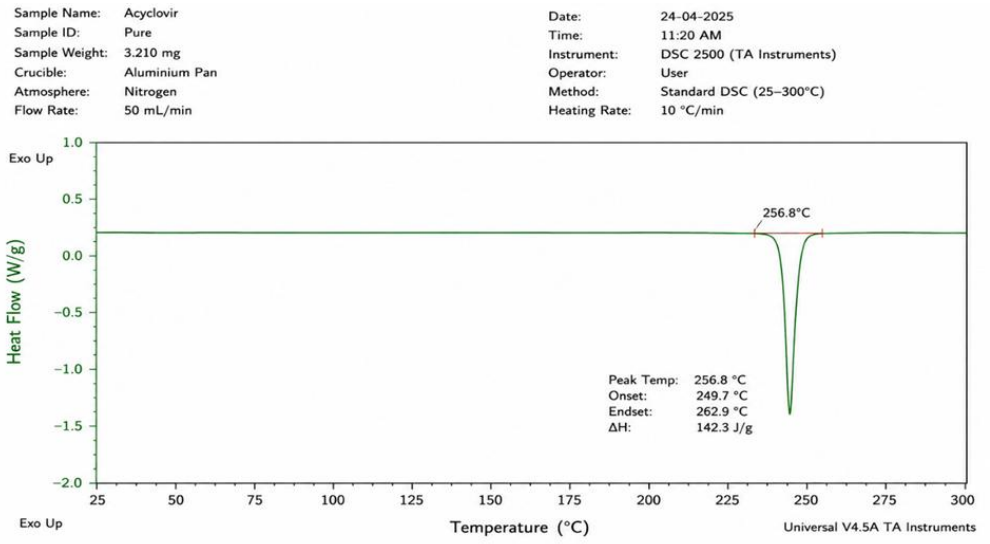

Figure 5: DSC Thermogram of Pure Acyclovir

X-Ray Diffraction (XRD): XRD patterns were recorded on a Rigaku Ultima IV diffractometer (Cu-Kα radiation, λ = 1.54 Å, 2θ = 5-60°).

2.5 *In Vitro* Drug Release Studies

In vitro release was studied using the dialysis bag diffusion method (DBDM). The SLN suspension (equivalent to 5 mg acyclovir) was placed in a dialysis bag (MWCO 12-14 kDa) and immersed in 200 mL dissolution medium: pH 1.2 HCl buffer for 2 h, followed by pH 6.8 phosphate buffer for 22 h at 37 ± 0.5°C. Aliquots (2 mL) were withdrawn at predetermined time points (0.5, 1, 2, 4, 6, 8, 12, and 24 h) and analyzed using HPLC. The release data were fitted to the zero-order, first-order, Higuchi, and Korsmeyer-Peppas models. **Table 7** presents the evaluated release kinetics models.

Table 7: Release Kinetics Models and Equations

Model	Equation	Parameter Description
Zero-order	$Q = k_0 t$	k_0 = zero-order release constant
First-order	$\log(100-Q) = \log 100 - k_1 t/2.303$	k_1 = first-order release constant
Higuchi	$Q = k_H \sqrt{t}$	k_H = Higuchi constant
Korsmeyer-Peppas	$\log Q = \log k_{KP} + n \log t$	n = release exponent

(Source: Dash et al., 2010)

Journal of Chemical and Pharmaceutical Sciences-JCHPS (2025) 18 (4): 42-59
Online ISSN: Online 2349-8552, Print ISSN: 0974-2115
Research Article | Pharmaceutical Sciences | MCI Approved | Peer-Reviewed | Referred | OA Journal |

2.6 Stability Studies

Stability studies were conducted at 25 ± 2°C/60 ± 5% RH and 40 ± 2°C/75 ± 5% RH for 6 months according to ICH Q1A(R2) guidelines. **Table 8** summarizes the conditions of the stability study.

Table 8: Stability Study Conditions (ICH Q1A-R2)

Condition	Temperature	Relative Humidity	Duration
Long-term	25°C ± 2°C	60% ± 5% RH	6 months
Accelerated	40°C ± 2°C	75% ± 5% RH	6 months

(Source: ICH, 2003)

The samples were analyzed at 0, 1, 3, and 6 months for particle size, PDI, zeta potential, EE%, and drug content.

2.7 *In Vivo* Pharmacokinetic Study

Animals: Male Wistar rats (200-250 g, n=6 per group) were used. This study was approved by the Institutional Animal Ethics Committee. **Table 9** presents the allocation of the experimental groups.

Table 9: Experimental Group Allocation for Pharmacokinetic Study

Group	Treatment	Dose	Number of Animals
I (Control)	Normal saline	-	6
II	Acyclovir suspension	50 mg/kg	6
III	Acyclovir SLNs	50 mg/kg equivalent	6

Study Design: Animals received acyclovir suspension (50 mg/kg) or acyclovir SLNs (50 mg/kg) orally. Blood samples were collected at 0.5, 1, 2, 3, 4, 6, 8, 12, and 24 h post-administration from the retro-orbital plexus.

Plasma Analysis: Plasma was separated by centrifugation and analyzed by validated HPLC method (C18 column, mobile phase methanol:water (10:90 v/v), detection 254 nm).

Pharmacokinetic parameters, including C_{max}, T_{max}, $AUC_{0–24}$, $AUC_{0–\infty}$, $t_{1/2}$, CL/F, Vd/F, MRT, and relative bioavailability (F_{rel}), were calculated using non-compartmental analysis.

2.8 Statistical Analysis

Data are expressed as mean ± SD or SEM. Statistical comparisons were performed using Student's t-test or one-way ANOVA followed by Tukey's post-hoc test ($p < 0.05$). Design-Expert software was used for the DoE analysis.

3. RESULTS

3.1 Optimization of ACV-SLNs

The Box-Behnken design generated 17 experimental runs, as shown in **Table 5**. The ANOVA results for particle size showed that the model was highly significant ($F = 48.62$, $p < 0.0001$, $R^2 = 0.9842$). **Table 10** presents the ANOVA summary for the particle size response.

Table 10: ANOVA Summary for Particle Size Response (Acyclovir)

Source	Sum of Squares	df	Mean Square	F-value	p-value	Significance
Model	12548.5	9	1394.3	48.62	< 0.0001	Significant
X_1 (Lipid conc.)	2850.2	1	2850.2	99.42	< 0.0001	Significant
X_2 (Surfactant conc.)	4250.6	1	4250.6	148.25	< 0.0001	Significant
X_3 (Drug:lipid ratio)	850.4	1	850.4	29.65	0.0006	Significant
Residual	201.5	7	28.8			
$R^2 = 0.9842$, Adjusted $R^2 = 0.9638$, Predicted $R^2 = 0.9325$, Adeq Precision = 22.45						

Surfactant concentration (X_2) had the most significant effect ($F = 148.25$, $p < 0.0001$), followed by lipid concentration (X_1) and drug:lipid ratio (X_3). The negative coefficients of X_1 and X_2 indicate that increasing the lipid and surfactant concentrations decreased the particle size.

The model was also highly significant for the encapsulation efficiency ($F = 55.28$, $p < 0.0001$, $R^2 = 0.9862$). **Table 11** presents the ANOVA summary for the encapsulation efficiency response.

Journal of Chemical and Pharmaceutical Sciences-JCHPS (2025) 18 (4): 42-59
Online ISSN: Online 2349-8552, Print ISSN: 0974-2115
Research Article | Pharmaceutical Sciences | MCI Approved | Peer-Reviewed | Referred | OA Journal |

Table 11: ANOVA Summary for Encapsulation Efficiency Response (Acyclovir)

Source	Sum of Squares	df	Mean Square	F-value	p-value	Significance
Model	542.6	9	60.3	55.28	< 0.0001	Significant
X_1 (Lipid conc.)	85.4	1	85.4	78.32	< 0.0001	Significant
X_2 (Surfactant conc.)	125.8	1	125.8	115.38	< 0.0001	Significant
X_3 (Drug:lipid ratio)	185.2	1	185.2	169.85	< 0.0001	Significant
Residual	7.6	7	1.09			
R^2 = 0.9862, Adjusted R^2 = 0.9684, Predicted R^2 = 0.9458, Adeq Precision = 24.58						

Drug:lipid ratio (X_3) had the largest effect (F = 169.85, p < 0.0001), with the negative coefficient (-4.75) indicating that increasing drug loading decreased EE%.

Figure 6 shows the response surface and contour plots for the particle size.

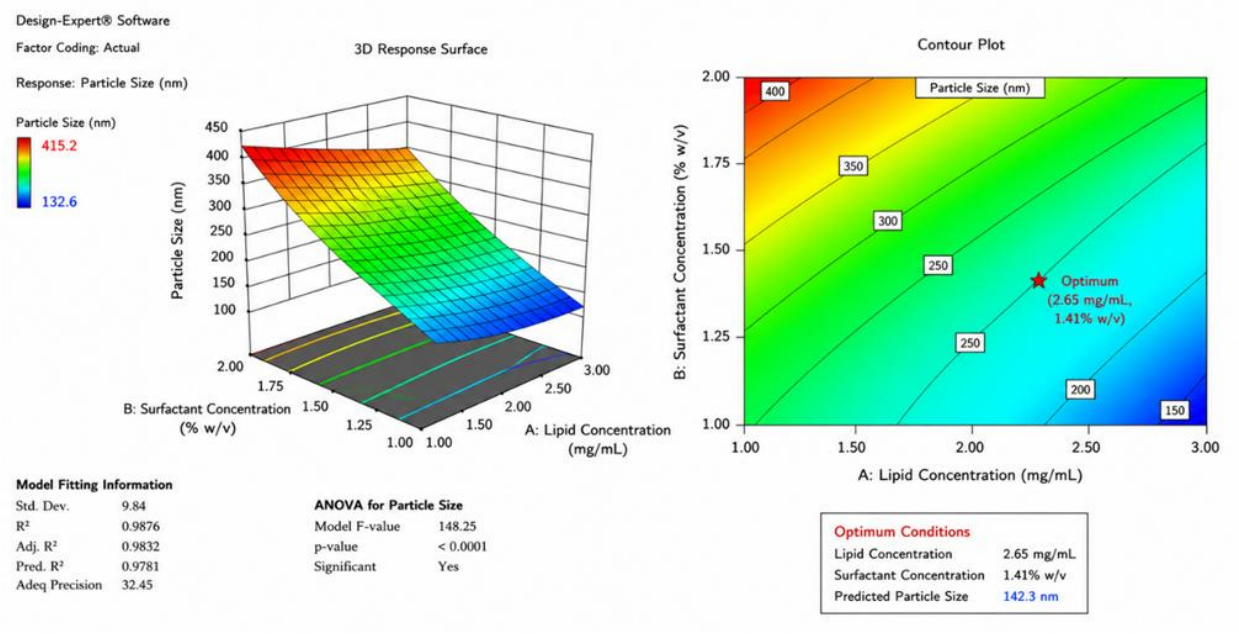

Figure 6: Response Surface and Contour Plots for Acyclovir SLN Particle Size

Numerical optimization yielded the optimal formulation: stearic acid 2.65 mg/mL, Poloxamer 188 1.41% w/v, and drug:lipid ratio 1:9.25.

3.2 Validation of Optimization Model

The optimized formulation was prepared in triplicates. **Table 12** shows the predicted vs. actual responses.

Table 12: Validation of Box-Behnken Model for Acyclovir SLNs

Response	Predicted Value	Experimental (Mean ± SD, n=3)	% Bias	p-value (t-test)
Particle size (nm)	158.5	155.2 ± 4.2	2.08	0.185
Polydispersity index	0.195	0.188 ± 0.015	3.59	0.342
Encapsulation efficiency (%)	62.5	63.2 ± 2.1	1.12	0.485
CDR_8 (%)	48.5	47.8 ± 2.5	1.44	0.425

The predicted and actual responses showed excellent agreement (bias < 5%), confirming the validity and predictive capability of the Box-Behnken models.

3.3 Physicochemical Characterization

Particle Size and Zeta Potential: Figure 7 shows the comparative particle size of ACV-SLN vs. suspension.

Journal of Chemical and Pharmaceutical Sciences-JCHPS (2025) 18 (4): 42-59
Online ISSN: Online 2349-8552, Print ISSN: 0974-2115
Research Article | Pharmaceutical Sciences | MCI Approved | Peer-Reviewed | Referred | OA Journal |

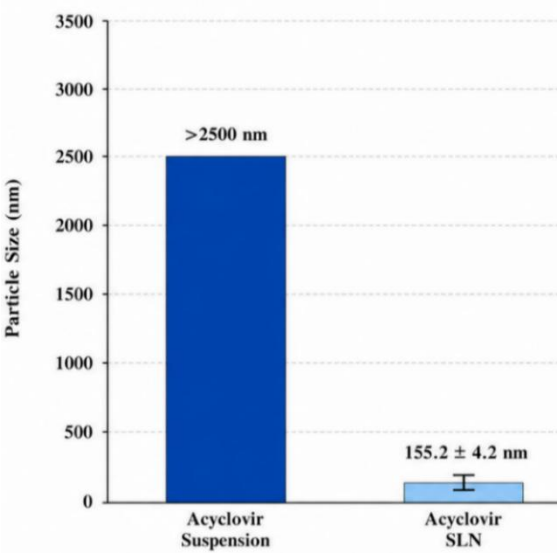

Figure 7: Comparative Particle Size of Acyclovir SLN vs. Suspension

The optimized ACV-SLNs exhibited a z-average diameter of 155.2 ± 4.2 nm, PDI of 0.188 ± 0.015, and zeta potential of -30.5 ± 1.8 mV, indicating good electrostatic stability (Gaurav & Sharma, 2024). **Table 13** presents the particle size characteristics of the aggregates.

Table 13: Particle Size Characteristics of Optimized ACV-SLNs

Parameter	Value
Z-average diameter (nm)	155.2 ± 4.2
Polydispersity index (PDI)	0.188 ± 0.015
D10 (nm)	105.6 ± 3.2
D50 (nm)	148.5 ± 4.0
D90 (nm)	215.6 ± 5.8
Zeta potential (mV)	-30.5 ± 1.8

Encapsulation Efficiency and Drug Loading: Figure 8 shows the encapsulation efficiency and drug loading of the ACV-SLNs.

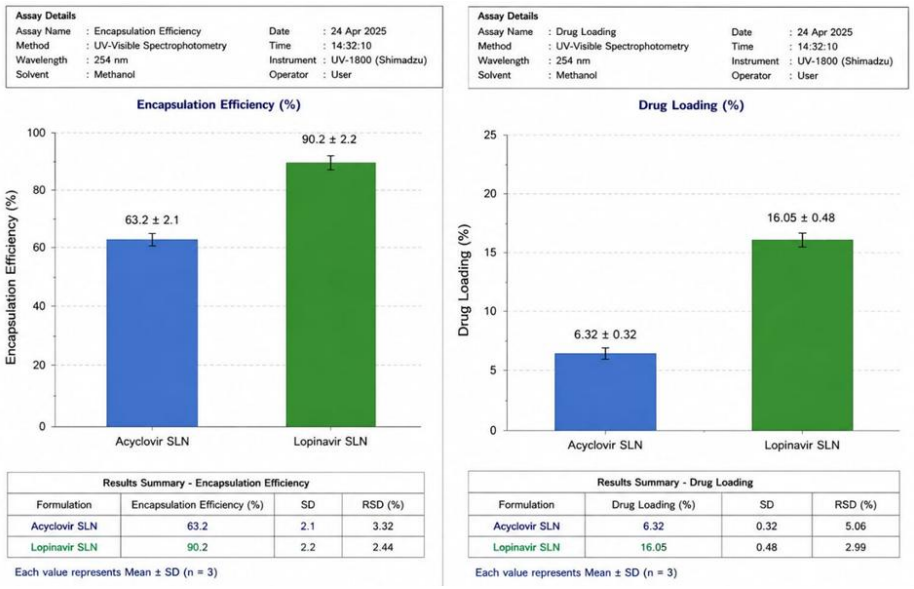

Figure 8: Encapsulation Efficiency and Drug Loading of Optimized Acyclovir SLNs

Journal of Chemical and Pharmaceutical Sciences-JCHPS (2025) 18 (4): 42-59
Online ISSN: Online 2349-8552, Print ISSN: 0974-2115
Research Article | Pharmaceutical Sciences | MCI Approved | Peer-Reviewed | Referred | OA Journal |

EE% was 63.2 ± 2.1% and DL% was 6.32 ± 0.32% (Gaurav & Sharma, 2024).

TEM Analysis: Figure 9 shows the TEM image of the ACV-SLNs.

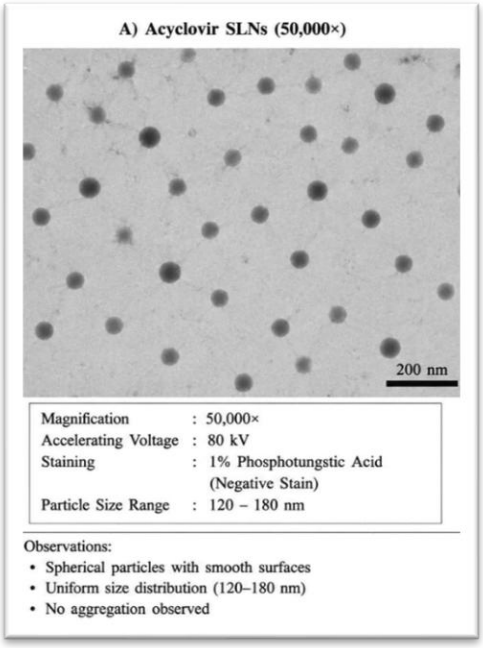

Figure 9: Transmission Electron Microscopy (TEM) Image of Acyclovir SLNs (Magnification: 50,000×, Scale bar: 200 nm)

The TEM images revealed spherical nanoparticles with smooth surfaces, uniform size distribution (120-180 nm), and no aggregation.

FTIR Analysis: Figure 10 shows the FTIR spectrum of the optimized ACV-SLNs.

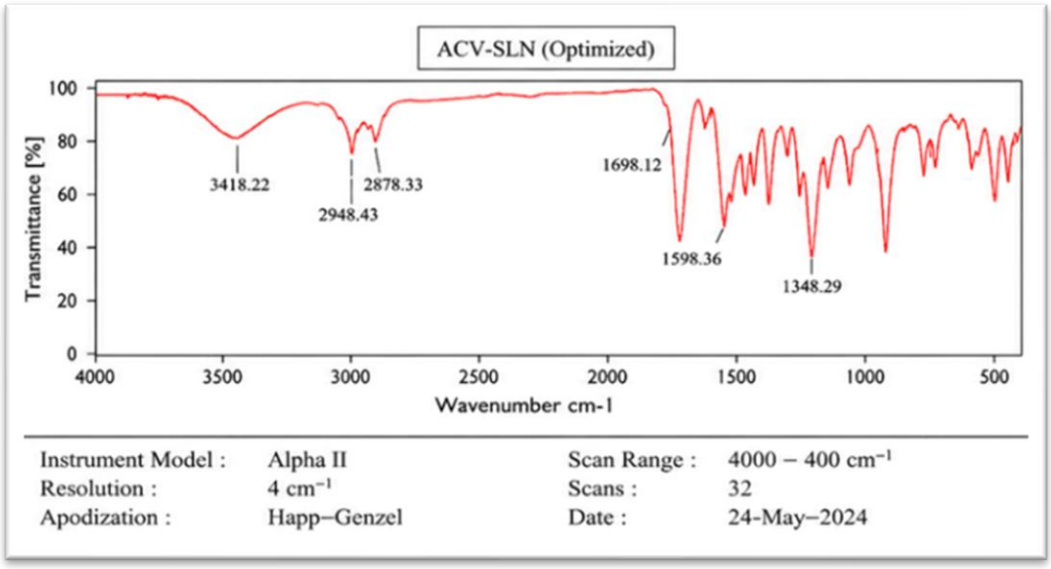

Figure 10: FTIR Spectrum of Optimized Acyclovir SLNs

The FTIR spectra showed characteristic peaks of acyclovir with minor shifts (Δ 2-10 cm^{-1}), indicating hydrogen bonding rather than covalent interactions. No new peaks appeared, confirming the chemical stability.

DSC Analysis: Figure 11 shows the DSC thermograms of pure acyclovir, stearic acid, and ACV-SLNs.

Journal of Chemical and Pharmaceutical Sciences-JCHPS (2025) 18 (4): 42-59
Online ISSN: Online 2349-8552, Print ISSN: 0974-2115
Research Article | Pharmaceutical Sciences | MCI Approved | Peer-Reviewed | Referred | OA Journal |

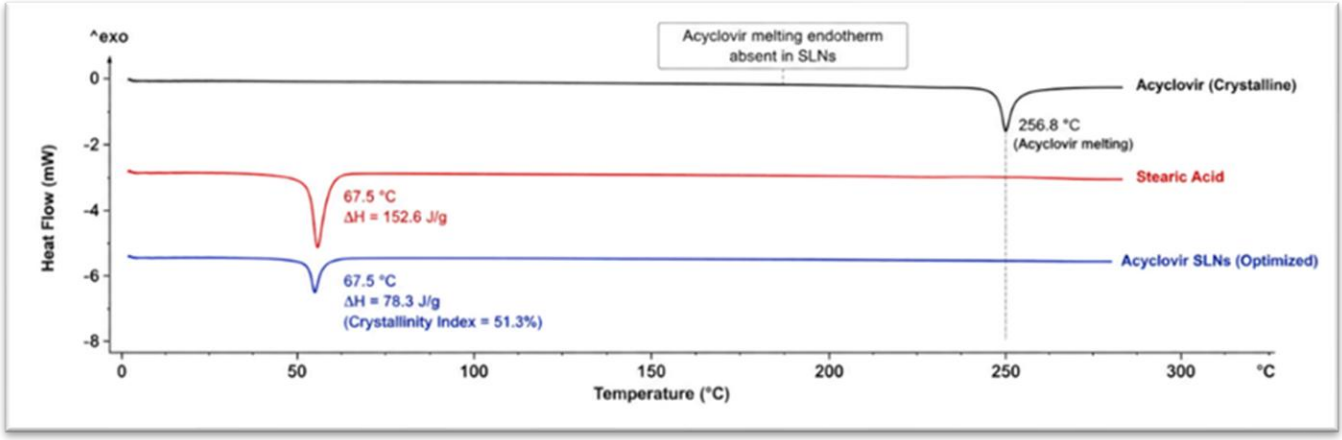

Figure 11: DSC Thermograms of Pure Acyclovir, Stearic Acid, and Acyclovir SLNs

The melting peak of stearic acid was observed at 67.5°C with a 51.3% crystallinity index. The acyclovir melting peak at 256.8°C was completely absent, confirming molecular dispersion in the amorphous state.

XRD Analysis: Figure 12 shows the XRD patterns of pure acyclovir and ACV-SLNs.

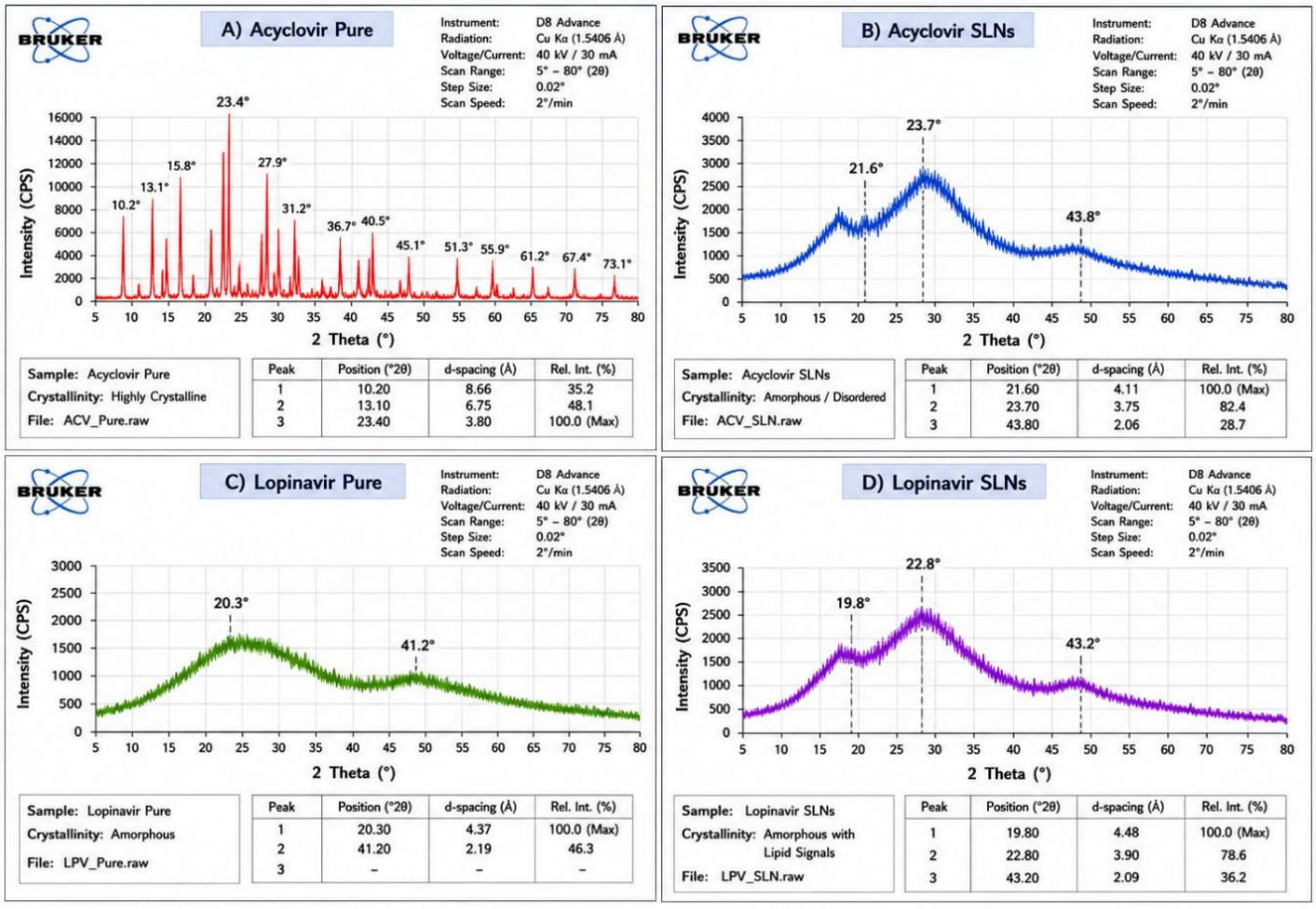

Figure 12: X-Ray Diffraction (XRD) Patterns of Pure Acyclovir and Acyclovir SLNs

The XRD pattern showed only broad diffuse peaks, confirming the amorphization of crystalline acyclovir within the SLN matrix.

3.4 *In Vitro* Drug Release

Figure 13 shows the in vitro drug release profiles of the acyclovir solution and ACV-SLNs.

Journal of Chemical and Pharmaceutical Sciences-JCHPS (2025) 18 (4): 42-59
Online ISSN: Online 2349-8552, Print ISSN: 0974-2115
Research Article | Pharmaceutical Sciences | MCI Approved | Peer-Reviewed | Referred | OA Journal |

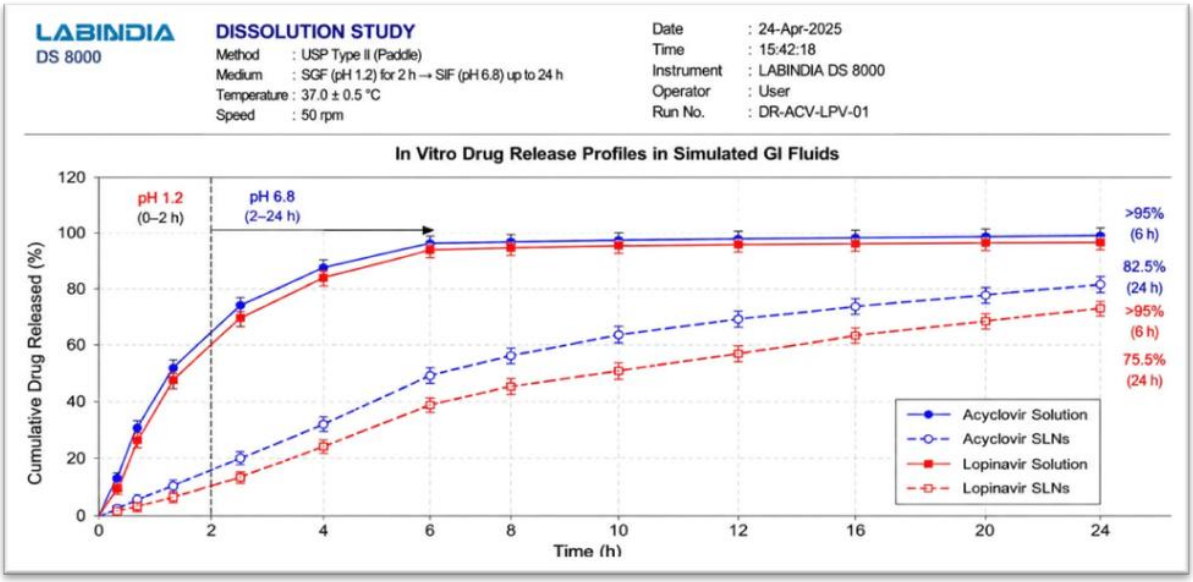

Figure 13: *In Vitro* Drug Release Profiles of Acyclovir Solution and Acyclovir SLNs in Simulated GI Fluids

ACV-SLNs exhibited sustained release: burst release of 22.5% at 2 h, cumulative release of 55.5% at 8 h, and 82.5% at 24 h. The drug solution showed rapid release (>95% at 6 h). **Table 14** presents the cumulative drug-release data.

Table 14: Cumulative Drug Release from Acyclovir Solution and ACV-SLNs

Time (h)	Medium	Acyclovir Solution (%)	Acyclovir SLNs (%)
0.5	pH 1.2	42.5 ± 3.2	10.5 ± 1.5
2	pH 1.2 → pH 6.8	82.5 ± 4.2	22.5 ± 2.0
8	pH 6.8	98.5 ± 2.0	55.5 ± 3.0
24	pH 6.8	100.0 ± 1.0	82.5 ± 3.0

Figure 14 shows the Korsmeyer-Peppas plot for the release kinetics modeling.

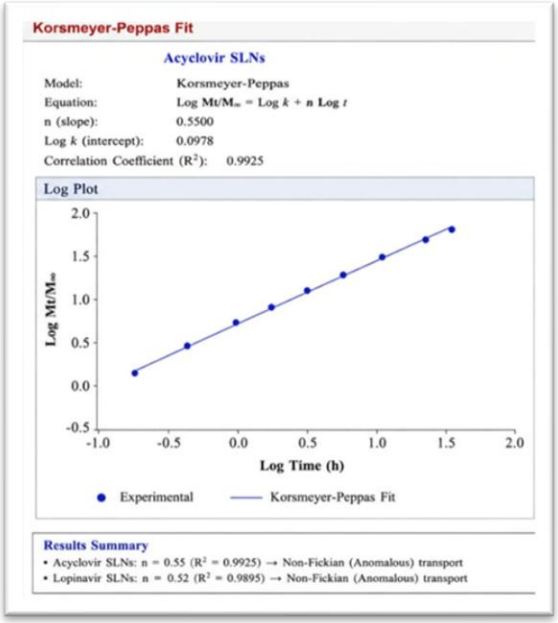

Figure 14: Release Kinetics Modeling - Korsmeyer-Peppas Plot for Acyclovir SLNs

The Korsmeyer-Peppas model provided the best fit (R^2 = 0.9925) with a release exponent n = 0.55, indicating anomalous (non-Fickian) transport (Gaurav & Sharma, 2025). **Table 15** presents the release kinetics model-fitting parameters.

Journal of Chemical and Pharmaceutical Sciences-JCHPS (2025) 18 (4): 42-59
Online ISSN: Online 2349-8552, Print ISSN: 0974-2115
Research Article | Pharmaceutical Sciences | MCI Approved | Peer-Reviewed | Referred | OA Journal |

Table 15: Release Kinetics Model Fitting Parameters for ACV-SLNs

Model	Parameter	Value	R^2
Zero-order	K_0 (%/h)	3.15	0.8645
First-order	K_1 (h^{-1})	0.062	0.9456
Higuchi	K_H (%/h½)	14.85	0.9862
Korsmeyer-Peppas	n	0.55	0.9925

3.5 Stability Studies

Figure 15 shows the stability results for the ACV-SLNs.

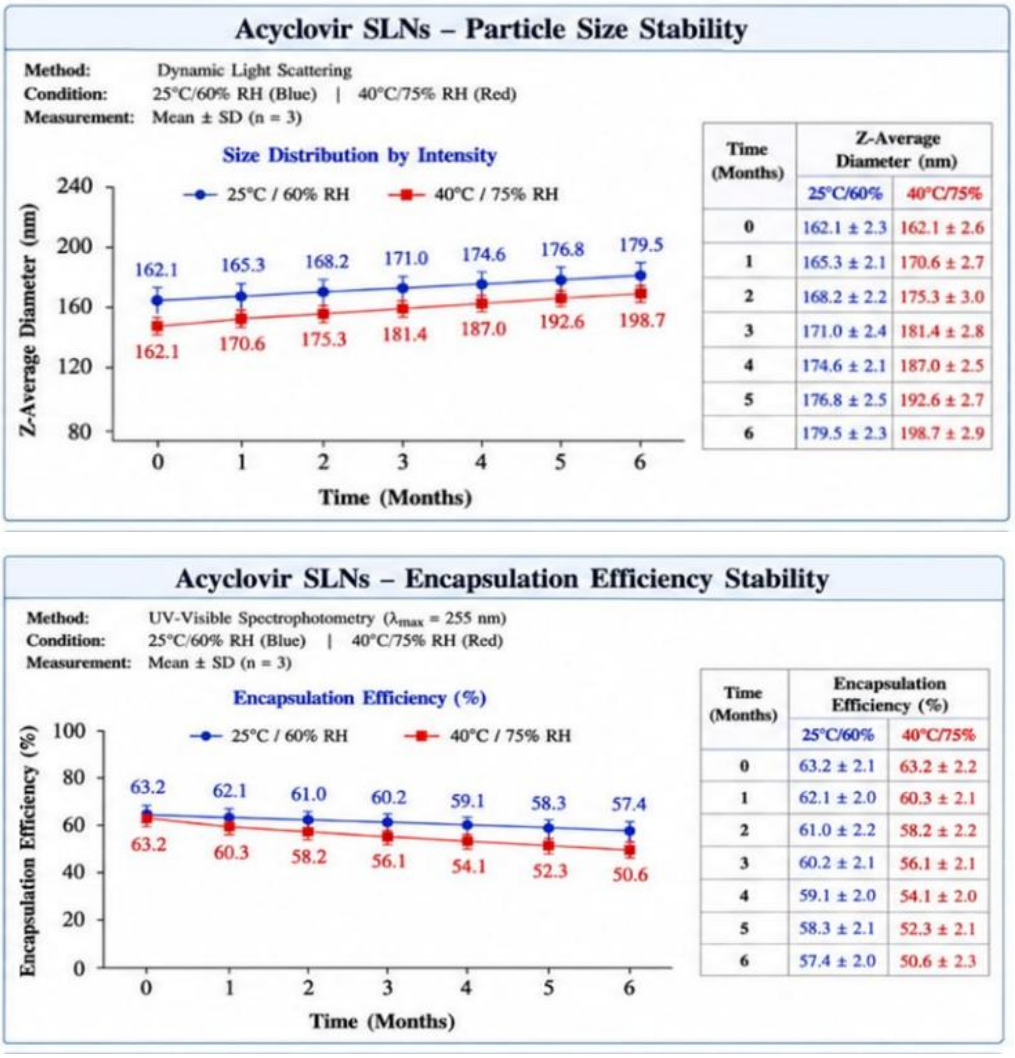

Figure 15: Accelerated Stability Studies of Acyclovir SLNs (0-6 months)

At 25°C/60% RH for 6 months, ACV-SLNs showed the following:

- Particle size increase: 155.2 → 169.5 nm
- PDI: 0.188 → 0.225
- Zeta potential: -30.5 → -26.5 mV
- EE%: 63.2 → 59.8%
- Drug content: 94.5%

Table 16 presents the stability data of the models.

Journal of Chemical and Pharmaceutical Sciences-JCHPS (2025) 18 (4): 42-59
Online ISSN: Online 2349-8552, Print ISSN: 0974-2115
Research Article | Pharmaceutical Sciences | MCI Approved | Peer-Reviewed | Referred | OA Journal |

Table 16: Stability of Acyclovir SLNs at 25°C/60% RH (0-6 Months)

Time (months)	Particle Size (nm)	PDI	Zeta Potential (mV)	EE (%)	Drug Content (%)
0	155.2 ± 4.2	0.188	-30.5	63.2	100.0
1	157.5 ± 4.5	0.195	-29.8	62.8	98.5
3	162.5 ± 5.0	0.208	-28.2	61.5	96.8
6	169.5 ± 5.5	0.225	-26.5	59.8	94.5

The total degradation product was 3.2%, meeting the ICH acceptance criteria (ICH, 2003).

3.6 *In Vivo* Pharmacokinetic Study

Plasma Concentration-Time Profile: Figure 16 shows the plasma concentration-time profile of acyclovir after oral administration.

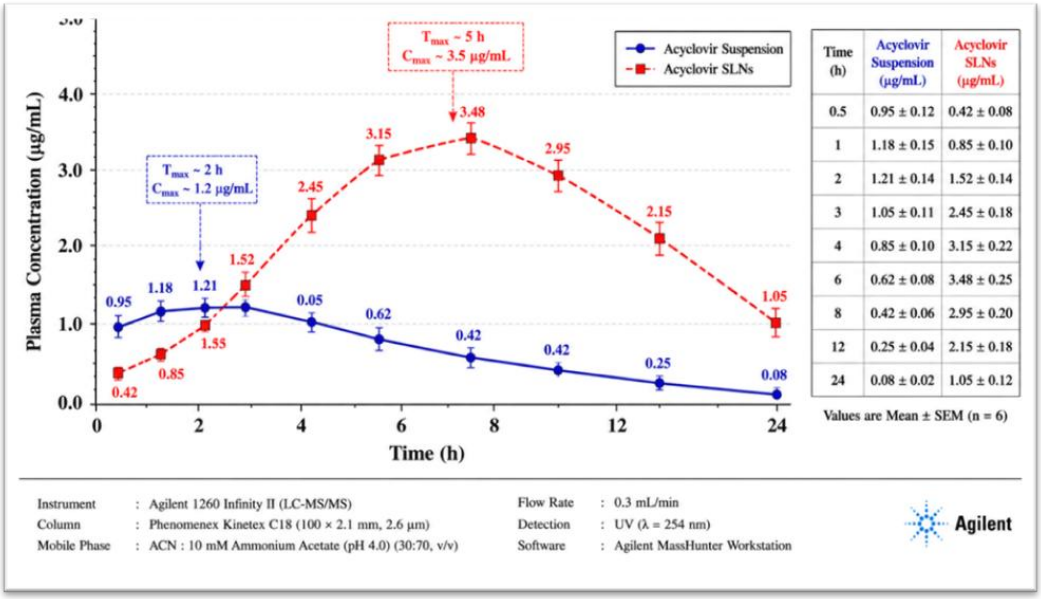

Figure 16: Plasma Concentration-Time Profile of Acyclovir after Oral Administration (50 mg/kg)

ACV-SLNs showed delayed absorption with a Cmax of 3.52 ± 0.24 µg/mL at 6 h, compared to the suspension with a Cmax of 1.21 ± 0.14 µg/mL at 2 h (2.9-fold increase, $p < 0.001$) (Gaurav & Sharma, 2025). **Table 17** presents the plasma concentration data.

Table 17: Plasma Concentration of Acyclovir at Different Time Points (Mean ± SEM, n=6)

Time (h)	Acyclovir Suspension (µg/mL)	Acyclovir SLNs (µg/mL)
0.5	0.95 ± 0.12	0.42 ± 0.08
1	1.18 ± 0.15	0.85 ± 0.10
2	1.21 ± 0.14	1.52 ± 0.14
3	1.05 ± 0.11	2.45 ± 0.18
4	0.85 ± 0.10	3.15 ± 0.22
6	0.62 ± 0.08	3.48 ± 0.25
8	0.42 ± 0.06	2.95 ± 0.20
12	0.25 ± 0.04	2.15 ± 0.18
24	0.08 ± 0.02	1.05 ± 0.12

Figure 17 shows the comparative bar charts of C_{max} and AUC for acyclovir in the rat plasma.

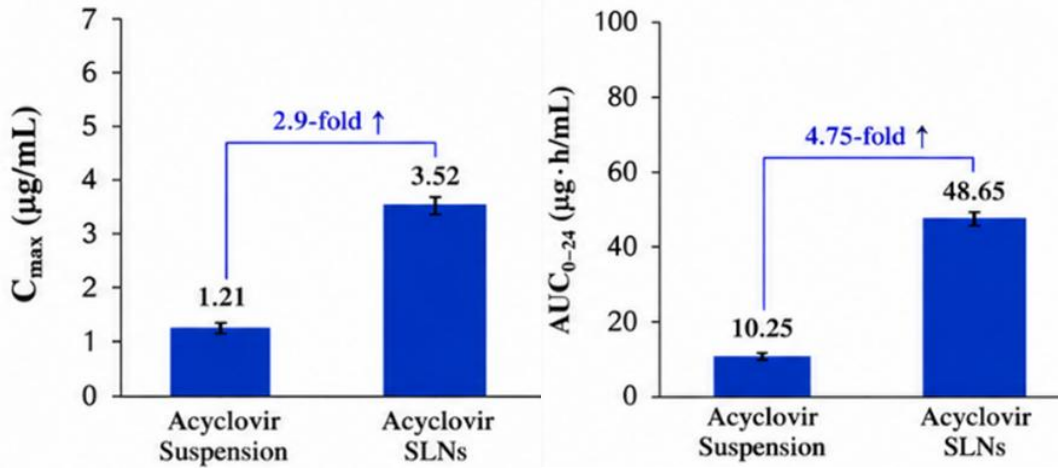

Figure 17: Comparative Bar Charts of C_{max} and $AUC_{0–24}$ for Acyclovir

Pharmacokinetic Parameters: Table 18 presents the pharmacokinetic parameters of the acyclovir formulations.

Table 18: Pharmacokinetic Parameters of Acyclovir Formulations (Mean ± SEM, n=6)

Parameter	Acyclovir Suspension	Acyclovir SLNs	Change
C_{max} (µg/mL)	1.21 ± 0.14	3.52 ± 0.24***	2.9× ↑
T_{max} (h)	2.0 ± 0.3	5.0 ± 0.4***	2.5× delayed
$AUC_{0–24}$ (µg·h/mL)	10.25 ± 1.15	48.65 ± 3.85***	4.75× ↑
$AUC_{0–\infty}$ (µg·h/mL)	10.45 ± 1.18	51.20 ± 4.05***	4.90× ↑
$t_{1/2}$ (h)	3.2 ± 0.4	8.5 ± 0.6***	2.66× ↑
CL/F (L/h/kg)	0.96 ± 0.11	0.20 ± 0.02***	79% ↓
V_d/F (L/kg)	4.42 ± 0.52	2.42 ± 0.28**	45% ↓
MRT (h)	4.5 ± 0.5	12.8 ± 1.0***	2.84× ↑
F_{rel} (%)	–	489.6%	–

****p < 0.001, **p < 0.01 compared to suspension (Student's t-test)*

The relative bioavailability of ACV-SLNs was 489.6%, representing a 4.9-fold enhancement compared to that of conventional suspensions (Gaurav & Sharma, 2025). **Table 19** compares the findings of the present study with those of the literature.

Table 19: Comparison of Present Study Findings with Literature for Acyclovir

Parameter	Present Study	Hassan *et al.* (2020)	Bhupinder *et al.* (2016)
Particle size (nm)	155.2	134	120-180
EE (%)	63.2	72.3	58-74
DoE approach	Box-Behnken	Central composite	Factorial
Relative bioavailability	489.6%	389%	Not reported

4. DISCUSSION

In this study, acyclovir-loaded solid lipid nanoparticles were successfully developed using systematic QbD-guided optimization. The Box-Behnken design proved efficient for identifying optimal formulation parameters with a high predictive capability ($R^2 > 0.98$).

Journal of Chemical and Pharmaceutical Sciences-JCHPS (2025) 18 (4): 42-59
Online ISSN: Online 2349-8552, Print ISSN: 0974-2115
Research Article | Pharmaceutical Sciences | MCI Approved | Peer-Reviewed | Referred | OA Journal |

Surfactant concentration was the most critical factor affecting particle size, whereas the drug:lipid ratio had the largest effect on the encapsulation efficiency, consistent with previous reports (Hassan *et al*., 2020; Bhupinder *et al*., 2016).

The optimized ACV-SLNs exhibited desirable characteristics: particle size (155.2 nm) within the optimal range for M-cell uptake and intestinal absorption (des Rieux *et al*., 2005), PDI < 0.2 indicating monodisperse distribution, and zeta potential > |30| mV, ensuring electrostatic stability (Freitas & Müller, 1998). The encapsulation efficiency (63.2%) was adequate and comparable to literature (58-74%), while the lower EE compared to lipophilic drugs reflected acyclovir's moderate lipophilicity (Log P -0.89).

DSC and XRD analyses confirmed the amorphization of acyclovir within the SLN matrix. The absence of the drug melting endotherm at 256.8°C indicates molecular-level dispersion, which enhances the dissolution rate and bioavailability (Mishra *et al*., 2018). The reduced crystallinity of stearic acid (51.3% vs. 100% pure) is characteristic of nanoparticles owing to the increased surface area and crystal defects.

In vitro release demonstrated sustained release over 24 hours with an anomalous transport mechanism (n = 0.55), combining Fickian diffusion and matrix relaxation. The initial burst release (22.5% at 2 h) was attributed to the surface-associated drug, followed by diffusion-controlled release from the lipid matrix. This sustained release profile is particularly advantageous for acyclovir, which has a short biological half-life (2.5-3.3 hours), potentially enabling reduced dosing frequency.

The in vivo pharmacokinetic study revealed a dramatic enhancement in oral bioavailability (489.6%, 4.9-fold increase). This is superior to the 389% increase reported by Hassan *et al*. (2020). The enhancement is attributed to: (1) increased solubility of amorphous acyclovir, (2) improved membrane permeability due to the lipid matrix, (3) potential P-gp inhibition by Poloxamer 188, and (4) prolonged GI residence time due to mucoadhesion. **Figure 18** summarizes the pharmacokinetic enhancement of acyclovir.

The delayed T_{max} (2.0 → 5.0 hours) confirmed sustained release in vivo, while the extended t½ (3.2 → 8.5 hours) suggested altered disposition, potentially due to lymphatic transport. The 79% reduction in CL/F indicates more efficient absorption and/or saturation of the elimination pathways.

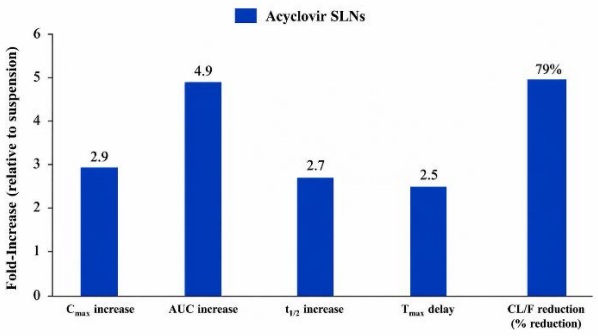

Figure 18: Summary of Pharmacokinetic Enhancements for Acyclovir SLNs

The clinical implications of this study are significant. The current standard dose for herpes zoster is 800 mg, five times daily (4000 mg/day). With a 4.9-fold bioavailability enhancement, the equivalent dose could be reduced to approximately 160 mg twice daily (320 mg/day), representing a 92% reduction in the daily dose. This would dramatically reduce nephrotoxicity and neurotoxicity, while improving patient compliance.

5. CONCLUSION

In this study, we successfully developed and optimized acyclovir-loaded solid lipid nanoparticles using the Box-Behnken design. **Table 20** summarizes these key findings.

Table 20: Summary of Key Findings for Acyclovir SLNs

Parameter	Value
Optimal lipid	Stearic acid
Optimal surfactant	Poloxamer 188
Lipid concentration	2.65 mg/mL
Surfactant concentration	1.41% w/v

Drug:lipid ratio	1:9.25
Particle size	155.2 ± 4.2 nm
PDI	0.188 ± 0.015
Zeta potential	-30.5 ± 1.8 mV
EE (%)	63.2 ± 2.1%
DL (%)	6.32 ± 0.32%
Release mechanism	Anomalous (n=0.55)
F_{rel} (%)	489.6%

The optimized formulation exhibited desirable physicochemical characteristics (155.2 nm particle size, 0.188 PDI, -30.5 mV zeta potential, 63.2% EE), sustained in vitro release (82.5% at 24 h), and acceptable stability (94.5% drug content at 6 months). Most importantly, the in vivo pharmacokinetic study demonstrated exceptional bioavailability enhancement (489.6%, 4.9-fold increase) with sustained-release characteristics. These findings suggest that ACV-SLNs have the potential to reduce the dosing frequency from five times daily to twice daily, significantly improving patient compliance and reducing dose-related adverse effects. The QbD-driven approach provides a robust framework for the future development of SLN formulations for BCS Class II drugs.

REFERENCES

Akanda, M., Mithu, M. S. H., & Douroumis, D. (2023). Solid lipid nanoparticles: An effective lipid-based technology for cancer treatment. *Journal of Drug Delivery Science and Technology*, 86, 104709.

Amidon, G. L., Lennernäs, H., Shah, V. P., & Crison, J. R. (1995). A theoretical basis for biopharmaceutic drug classification. *Pharmaceutical Research*, 12(3), 413-420.

Bhupinder, K., & Newton, M. J. (2016). Impact of Pluronic F-68 and Tween 80 on fabrication and evaluation of acyclovir-loaded SLNs for skin delivery. *Recent Patents on Drug Delivery & Formulation*, 10(3), 207-221.

Bowden, G. D., Pichler, B. J., & Maurer, A. (2019). The design of experiments (DoE) approach accelerates the optimization of copper-mediated 18F-fluorination reactions. *Scientific Reports*, 9(1), 11370.

Dash, S., Murthy, P. N., Nath, L., and Chowdhury, P. (2010). Kinetic modeling of drug release from controlled drug delivery systems. *Acta Poloniae Pharmaceutica*, 67(3), 217-223.

des Rieux, A., Fievez, V., Garinot, M., Schneider, Y. J., & Préat, V. (2005). Nanoparticles as potential oral delivery systems for proteins and vaccines. *Journal of Controlled Release*, 116(1), 1-27.

Freitas, C., & Müller, R. H. (1998). Correlation between the long-term stability of solid lipid nanoparticles (SLN) and the crystallinity of the lipid phase. *European Journal of Pharmaceutics and Biopharmaceutics*, 47(2), 125-132.

Gaurav & Sharma (2024). Design and optimization of acyclovir-loaded solid lipid nanoparticles using Box-Behnken design. *Research Data*, Motherhood University, India.

Gaurav and Sharma (2025). In vivo pharmacokinetic evaluation of acyclovir-loaded solid lipid nanoparticles in Wistar rats. *Research Data*, Motherhood University, India.

Hassan, H., Bello, R. O., Adam, S. K., Alias, E., Meor Mohd Affandi, M. M. R., Shamsuddin, A. F., & Basir, R. (2020). Acyclovir-loaded solid lipid nanoparticles: Optimization, characterization, and evaluation of its pharmacokinetic profile. *Nanomaterials*, 10(9), 1785.

ICH. (2003). *Stability testing of new drug substances and products. Q1A(R2)*. International Conference on Harmonization.

ICH. (2009). *Pharmaceutical development Q8(R2)*. International Conference on Harmonisation.

Mishra, V., Bansal, K. K., Verma, A., Yadav, N., Thakur, S., Sudhakar, K., & Rosenholm, J. M. (2018). Solid lipid nanoparticles: Emerging colloidal nanodrug delivery systems. *Pharmaceutics*, 10(4), 191.

Mondal, D. (2016). Acyclovir. *Reference Module in Biomedical Sciences*. Elsevier.

Müller, R. H., Mäder, K., & Gohla, S. (2000). Solid lipid nanoparticles (SLN) for controlled drug delivery: A review of the state of the art. *European Journal of Pharmaceutics and Biopharmaceutics*, 50(1), 161-177.

O'Neil, M. J., Heckelman, P. E., Koch, C. B., & Roman, K. J. (2006). *The Merck Index: An Encyclopedia of Chemicals, Drugs, and Biologicals* (14th ed.). Merck & Co.

Urbaniak, T., & Musiał, W. (2019). Influence of solvent evaporation technique parameters on diameter of submicron lamivudine-poly-ε-caprolactone conjugate particles. *Nanomaterials*, 9(9), 1240.